Aggregation Properties of the Chromonic Liquid Crystal Benzopurpurin 4B

Christopher B. McKitterick,[†] Nathaniel L. Erb-Satullo,[†] Nicholas D. LaRacuente,[†] Alexandra J. Dickinson,[†] and Peter J. Collings*[,†,‡]

Department of Physics & Astronomy, Swarthmore College, Swarthmore, Pennsylvania 19081, and Department of Physics and Astronomy, University of Pennsylvania, Philadelphia, Pennsylvania 19014

Received: October 23, 2009; Revised Manuscript Received: December 29, 2009

Optical polarization, absorption, and scattering studies along with confocal microscopy reveal that Benzopurpurin 4B forms aggregates of micrometer size at very low concentrations in aqueous solution. A chromonic liquid crystal phase is stable at room temperature down to concentrations as low as 0.4 wt %, which can only be possible if the aggregates contain an ample amount of water. The kinetics of aggregate formation are extremely slow, with changes going on for days before equilibrium is reached. The stacking free energy change is estimated to be $10.3 \pm 0.4\ k_BT$, which is in the higher range of values for recently studied chromonic liquid crystals. However, the very low concentration of the liquid crystal phase puts it in a different class, probably more similar to Scheibe or Jelly aggregates than the typical chromonic systems that are formed by simple stacks of molecules.

Introduction

Although it has been known for a long time that many dyes spontaneously aggregate in aqueous solutions and form chromonic liquid crystal phases at concentrations in the range 6−30 wt % (see reviews by Lydon[1,2]), only recently has the pace of research into these materials increased to the point that an understanding of some features is starting to emerge. A recent analysis that used the same techniques to examine both published and new experimental results emphasized that all chromonic liquid crystal systems show an X-ray diffraction peak due to the stacking of molecules 3.4 Å apart and a change in the absorption spectrum due to aggregation at concentrations well below those required for formation of the liquid crystal phase.[3] The report goes on to explain how the X-ray measurements consistently point to stacking in one dimension with the cross-sectional area of the stacks being close to one, two, three, or six molecular areas. Finally, it is explained that if the absorption change is used to estimate a stacking free energy change, among compounds that have the same aggregate structure, those with a higher stacking free energy change form a liquid crystal phase at lower concentrations.

Other very recent work has examined how the aggregation process responds to the presence of various salts and pH-altering agents,[4] and whether water molecules or counterions are tightly bound to the aggregates.[5] There is recent evidence that these aggregates can grow into worm-like micelles,[6] and both the liquid crystal phase[7] and the dried films from these materials[8,9] have recently been investigated for their unique optical properties. Finally, recent NMR and X-ray measurements indicate that the stacking of molecules may possess an alternation in the orientation of the individual molecules.[5,10]

There is another thread of investigation into aggregating dyes that is nearly as old. Examples of these systems tend to be compounds that form very large and more complicated aggregates at low concentrations. In some cases, a chromonic liquid crystal phase forms at higher concentrations, but in other cases the aggregates precipitate without a liquid crystal phase forming. These aggregates are known as Scheibe or Jelly (J-) aggregates and are characterized by the appearance of an intense, narrow absorption peak due to aggregation.[11] The most studied example of this class of compounds is pseudoisocyanine, which possesses a liquid crystal phase at concentrations as low as 0.4 wt %.[12] Static light scattering and cryo-TEM investigations on pseudoiscyanine aggregates with added salt yield length measurements on the order of a third of a micrometer.[12,13] On the other hand, a water-soluble derivative of porphyrin forms large aggregates (roughly a micrometer in length) at concentrations as low as 0.0002 wt % but precipitates before forming a liquid crystal phase.[14] There is cryo-TEM evidence in both the aggregating dye systems and J-aggregate systems that at high concentration and/or with added salt, additional organization of the aggregates takes place, forming bundles, fibers, or ribbons.[15,16]

Unlike the aggregating dye systems that show a reduction in the absorption coefficient but only a slight change in the shape of the absorption spectrum as the concentration is increased, aggregation in the systems forming J-aggregates usually results in a drastic change in the absorption spectrum in addition to the reduction in the absorption coefficient. Often this change is the appearance of a narrow, red-shifted peak in the absorption spectrum with increasing concentration.[12,17] This spectral change is usually explained by molecular exciton theory (see ref 18 as an example), which indicates that adjacent molecules in the aggregate are laterally displaced from one another.

The two different investigative threads have also described the aggregation process differently. In aggregating dye systems, isodesmic aggregation is a common starting point. In this type of process, aggregation occurs at all concentrations, with a distribution of very small aggregates forming at lower concentrations and with a steady shift of the distribution to larger aggregates as the concentration is increased.[10] For the J-aggregates, it is often suggested that the assembly of large aggregates begins at a specific concentration (the critical micelle concentration or cmc). Yet in both of these systems, there is

* To whom correspondence should be addressed. E-mail: PCOLLIN1@swarthmore.edu. Phone: (610) 328-7791. Fax: (610) 328-7895.
† Swarthmore College.
‡ University of Pennsylvania.

10.1021/jp910136p
Published on Web 01/20/2010

evidence that both approaches are too simplistic, with evidence for a cmc in an aggregating dye system[19] and evidence for dimer formation in systems of J-aggregates.[12]

Clearly there are common elements in the behavior of the two types of systems, and researchers in one area can learn a great deal from investigators in the other area. It is already known that the cyanine dyes span both types of systems, with some possessing a columnar nematic phase and with others showing a sheet-like smectic phase.[20] From this perspective, the textile dye Benzopurpurin 4B (Direct Red 2) is an interesting case. There are references to early investigations stating that aggregation only occurs in the presence of added electrolyte.[21] The structure of Benzopurpurin 4B resembles many aggregating dyes, yet there is more recent evidence that it forms a liquid crystal phase at concentrations as low as 0.34 wt %.[22] These researchers observed a broad peak in the specific heat at the temperature the liquid crystal phase formed, and the transition temperature increased as the concentration increased. NMR relaxation measurements also indicated that aggregation resulted in some of the water being "bound", probably incorporated into the aggregates in some fashion.

The unusual combination of a molecular structure reminiscent of the aggregating dyes and a low concentration for liquid crystal phase formation typical of J-aggregate systems provides ample motivation for a careful investigation of Benzopurpurin 4B (BPP 4B). This includes a determination of its phase diagram, a study of how its absorption spectrum changes with an increase in concentration, an X-ray diffraction measurement to see if molecular stacking is present, a light scattering investigation to gauge the size of the aggregates, an attempt to image the aggregates using confocal microscopy, and finally an exploration of theoretical explanations that might be capable of explaining the behavior of BPP 4B. The results indicate that BPP 4B possesses unusual properties, some of which are shared with aggregating dye systems, and others of which are typical of systems of J-aggregates. The transition temperature from the liquid crystal phase to the isotropic liquid phase increases with concentration, but unlike aggregating dye systems, there is no distinct interface between the liquid crystal phase and the isotropic liquid phase. The addition of sodium chloride increases the transition temperature, but only for salt concentrations over 0.3 wt %. The absorption coefficient decreases as the concentration is increased, similar to what happens in aggregating dyes (i.e., there is no additional red- or blue-shifted peak that occurs due to aggregation). Analysis of the absorption spectra yields a stacking free energy change that is toward the top of the range of estimates for aggregating dyes. But unlike aggregating dyes and very much like J-aggregates, light scattering measurements of samples with a concentration below what is necessary to form the liquid crystal phase indicate a wide distribution of large aggregates (of micrometer size). The confocal microscope images of aggregates immobilized because they are probably stuck to the glass surface confirm the light scattering results, in that a wide variety of aggregate lengths are observed with the average around 2.5 μm. Interestingly, the widths of the aggregates are much smaller than the lengths and below the resolution limit of the confocal microscope.

Aggregation Theory

The most simple theories that have been proposed for aggregating systems are based on a free energy difference between molecules in solution and molecules in an aggregate. Sometimes this difference is referred to as the "stacking free energy change" and sometimes it is called the "scission free energy". The fundamental physics behind these theories is on one hand that attractive interactions between molecules in an aggregate plus hydrophobic effects favor aggregation, or on the other hand that the ends of the aggregates cost more free energy because of both hydrophobic effects and a less favorable arrangement of the molecules compared to the interior of the aggregate. If these basic ideas are combined with a requirement that the aggregate must contain a specific number of molecules, then a sharp critical micelle concentration is predicted, as has been observed in the case of spherical micelles. If the number of molecules in an aggregate is unconstrained, then one theoretical result is that the aggregation is isodesmic, meaning that some aggregation takes place at all concentrations, with the distribution of aggregate size tending toward larger and larger aggregates as the concentration increases. In this system, a critical micelle concentration can be defined when half of the molecules are monomers in solution, but the transition from many monomers to few monomers is very broad.

It is not difficult to formulate a theory that covers a wider range of phenomena than the most simple ones. An example of this is described by Gelbart and Ben-Shaul in a review article.[23] In this theory, a free energy difference for all the molecules in an aggregate of i molecules relative to i molecules in solution $\Delta\mu_i$ contains two terms,

$$\frac{\Delta\mu_i}{k_B T} = -(i - 1)\alpha + (\delta - \alpha) \tag{1}$$

where α and δ are free energy parameters in units of $k_B T$, k_B is the Boltzmann constant, and T is the temperature. The parameter α represents the "stacking free energy change" and $\delta - \alpha$ represents the "scission free energy" (the free energy difference between the two ends of an aggregate relative to the two sides of a molecule). For this theory to describe systems such as the aggregating dyes and J-aggregates, δ must be greater or equal to α.

If this expression for the free energy of an aggregate is used to calculate the equilibrium distribution of aggregate sizes (see ref 10 for a description of how this typically is done), the following relationship is found between the volume fractions of aggregates of different size χ_i,

$$\chi_i = i(z\chi_1)^{i-1} e^{\alpha-\delta}\chi_1 \tag{2}$$

The parameter z is equal to $(L^3/V)e^{\alpha}$, where L^3/V is the appropriate factor stemming from a consideration of phase space and the external degrees of freedom of the molecules (V is the sample volume). For simplicity, many theories set L^3/V equal to v/V, where v is the volume of a single molecule. Note that eq 2 cannot be used as an expression for χ_1. With this relationship between the volume fractions of different size aggregates, the calculation can be completed in terms of the total volume fraction of the dye ϕ, because

$$\phi = \sum_{i=1}^{\infty} \chi_i \tag{3}$$

Thus given values for α, δ, T, and ϕ, values for the χ_i can be found using eqs 2 and 3.

Since the theory does not constrain the number of molecules in an aggregate, the solution always is a distribution of aggregate

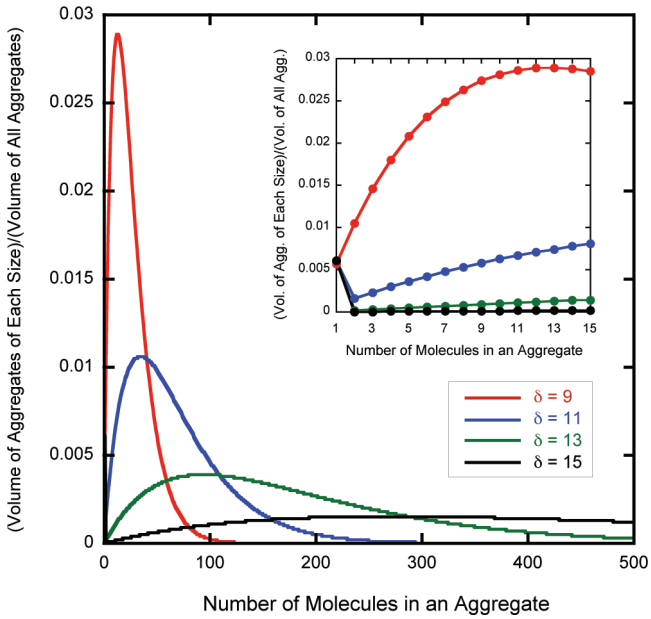

Figure 1. Distribution of aggregate size for four values of the free energy parameter δ. The dye volume fraction ϕ equals 0.02 and the free energy parameter α equals 9. The inset is an enlargement showing in detail the distributions for small aggregates. The average aggregate size is close to the distribution peaks, and is approximately given by eq 4. The dye volume fraction is much greater than the critical micelle volume fraction, so the fraction of monomers is saturated at about 0.005 in all four cases. The $\delta = 9$ curve represents isodesmic aggregation.

sizes. This is shown in Figure 1 in which the different distributions represent different values of the parameter δ. If $\delta \gg \alpha$, then there is a simple approximate expression for the average aggregate size $\langle i \rangle$,

$$\langle i \rangle = \frac{\sum_{i=1}^{\infty} i(\chi i/i)}{\sum_{i=1}^{\infty} (\chi i/i)} \approx \sqrt{\phi} e^{\delta/2} \qquad (4)$$

where (L^3/V) has been set to v/V. If instead of the fraction of total dye volume fraction, the fraction of the total number of aggregates is plotted, the distribution is proportional to χ_i/i and is approximately an exponential, varying as exp $(-i/\langle i \rangle)$.

Figure 2 shows the critical micelle concentration region for different values of the parameters α and δ. Again, if $\delta \gg \alpha$, there is a simple approximation for the critical micelle volume fraction, ϕ_C,

$$\phi_C \approx e^{-\alpha} \qquad (5)$$

This expression gives 0.000 34, 0.000 12, and 0.000 05 for the critical micelle volume fraction for the curves in the left-hand figure of Figure 2, which is the point at which each curve starts to decrease from one.

This more general theory has two limiting cases. The first is when $\delta = \alpha$. Only one term is present in the free energy expression, implying that the change in free energy for a molecule joining an aggregate is independent of aggregate size. This is called isodesmic aggregation and seems to apply to some of the aggregating dye systems. This case is illustrated by one curve in both Figures 1 and 2. The second limiting case is when $\delta \gg \alpha$. The change from mostly molecules in solution to mostly aggregates is sharp and the average aggregate size tends to be large. This is the case in which eqs 4 and 5 hold, and corresponds to the curves with the largest δ values in Figures 1 and 2.

Experimental Procedures and Results

Purification. Benzopurpurin 4B, the structure of which is given in Figure 5, was purchased from Sigma-Aldrich in a form that contained additional salts. After dialysis with water, ion chromatography of the water revealed that most of the additional salt was sodium chloride, and that the additional salts comprised approximately 50 wt % of the sample. Dialysis was then used to purify the material, first three times using a sodium chloride solution, and then three times using water.

To be able to measure the concentration of BPP 4B solutions used in the investigation, some of the dialyzed BPP 4B solution was lyophilized, and a known amount of the remaining powder was used to make a solution of known concentration. The absorption spectrum of this solution and numerous dilutions of this solution were measured, and the peak absorption recorded for each. A plot of the peak absorbance divided by the path length versus concentration was made, resulting is a slightly nonlinear relationship. As will be seen later, the nonlinearity is due to the fact that the absorption coefficient is concentration dependent. Once this calibration relationship was established, the concentration of any BPP 4B solution could be obtained by sufficiently diluting it, measuring the absorbance for a known path length, and using the calibration relationship to determine the concentration.

Phase Diagram. BPP 4B solutions of high enough concentration display birefringence, appearing bright when viewed through a polarizing microscope. The texture is mottled and shows no clear defects that might help identify which liquid crystal phase it is. When these solutions are heated, the brightness starts to decrease at a certain temperature, becoming zero at another temperature. Distinct regions showing the coexistence of two phases are not visible; rather, the bright parts of the mottled texture simply grow darker. This transition from a birefringent to nonbirefringent material was interpreted as the liquid crystal to isotropic liquid transition and, as is the case for all chromonic liquid crystals, was quite broad. To measure this transition as precisely as possible, a 120 μm thick sample of BPP 4B was placed between crossed polarizers and illuminated by a He−Ne laser and chopper arrangement. The transmitted light was collected by a photodiode connected to a lock-in amplifier that used the signal from the chopper as its reference.

A plot of the transmitted intensity vs sample temperature is shown in the inset of Figure 3. The data were fit to a Fermi function with the adjustable parameters being the maximum intensity I_0, the temperature at the midpoint of the transition T_0, and the temperature half-width of the transition ΔT

$$I(T) = \frac{I_0}{e^{(T-T_0)/\Delta T} + 1} \qquad (6)$$

The beginning and end of the transition were approximated by calculating two half-widths below and above the midpoint temperature (corresponding to 88% and 12% of the transition). These are plotted in Figure 3, where it is clear that the liquid crystal phase exists at room temperature at concentrations as

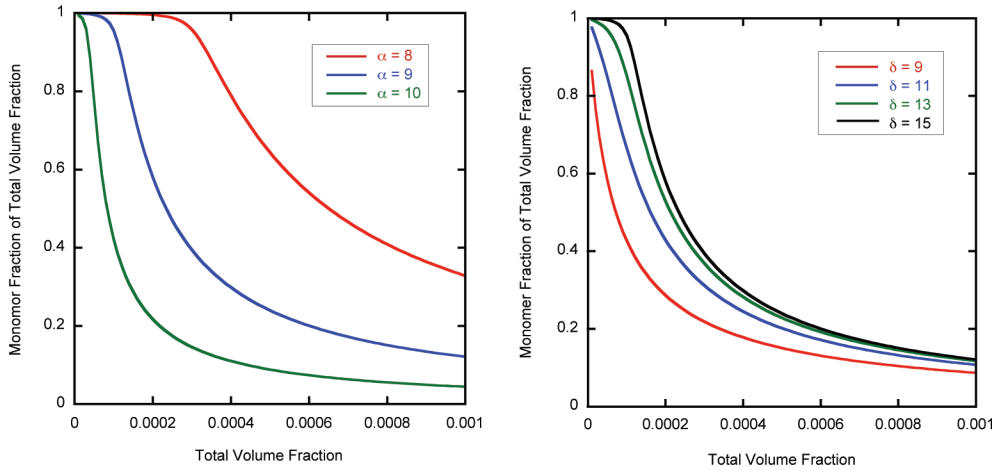

Figure 2. Monomer fraction of the total volume fraction of dye as a function of total volume fraction of dye. The free energy parameter δ equals 15 in the left-hand figure and the free energy parameter α equals 9 in the right-hand figure. Notice that the critical volume fraction strongly depends on α as implied by eq 5. The curve for which $\alpha = \delta$ represents isodesmic aggregation.

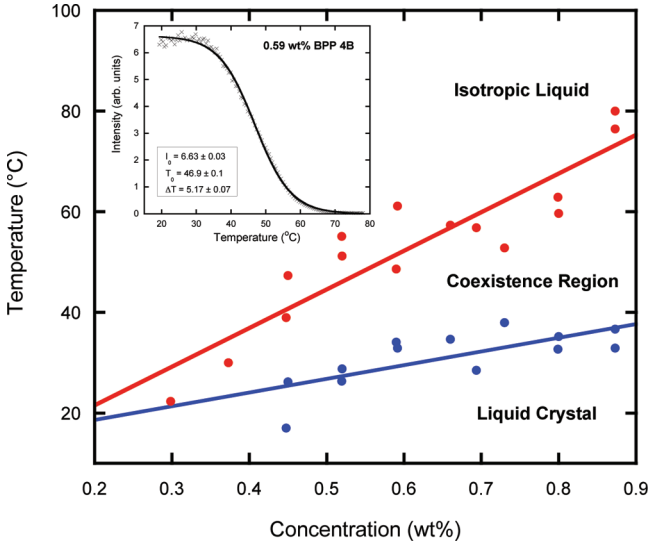

Figure 3. Phase diagram of BPP 4B. The inset shows the decrease in transmitted intensity as the temperature is increased, along with the fit to eq 6. As explained in the text, temperatures approximating the liquid crystal to coexistence region transition and coexistence region to isotropic liquid can be determined from the fit parameters. These are shown, with linear least-squares fits drawn to aid the eye.

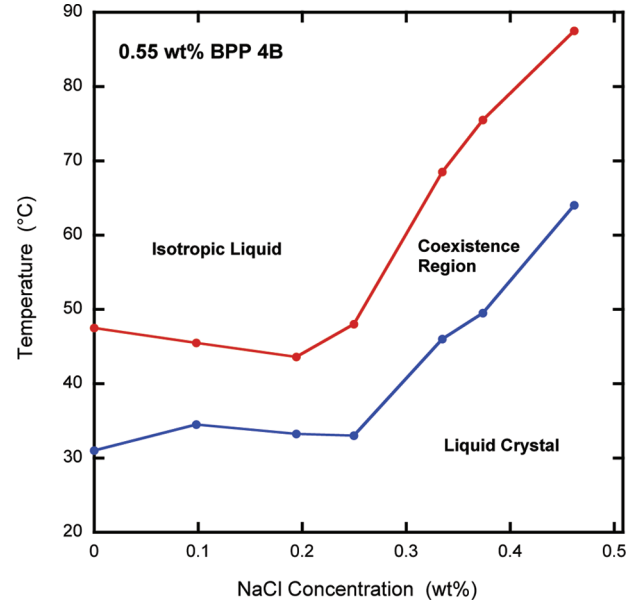

Figure 4. Liquid crystal to isotropic liquid transition in BPP 4B as a function of salt concentration. The BPP 4B concentration was 0.55 wt %.

low as 0.4 wt %, and that the transition gets broader as the concentration increases.

The transition was also examined for a 0.55 wt % BPP 4B sample with various concentrations of sodium chloride. As evident from Figure 4, the transition is not affected by the presence of salt until the concentration of sodium chloride reaches about 0.3 wt %, at which point the transition temperature increases. The width of the transition region remains roughly the same.

Absorption. Absorption measurements were made using a Cary 50 Bio UV−vis spectrophotometer for a wide range of BPP 4B concentrations in which the isotropic liquid is stable at room temperature. These concentrations ranged from a very dilute solution to a sample that was close to forming the liquid crystal phase. Different path lengths were utilized to keep the absorbance in a suitable range for the spectrophotometer. Figure 5 shows the results. As the concentration increases, the absorption coefficient in the middle of the visible absorption band decreases while the absorption coefficient at the high end of the visible spectrum increases. The shape of the visible absorption band does not change drastically, and an isosbestic point appears to be present around 560 nm.

The presence of sodium chloride decreases both the maximum absorption coefficient and the wavelength of maximum absorption. The effect is small until the sodium chloride concentration reaches about 0.3 wt %, after which the maximum absorption coefficient decreases and the wavelength of maximum absorption decreases slightly (see Figure 6). The addition of more salt again has little effect, until at roughly 0.8 wt % changes similar to the ones at 0.3 wt % occur. At higher concentrations up to 2.0 wt %, no further changes take place.

Light Scattering. Dynamic light scattering measurements were made with a Brookhaven Instruments BI-9000AT light scattering system equipped with a TurboCorr digital autocorrelator. To avoid the absorption band of BPP 4B as much as possible, 647 nm light from a Coherent Innova 70 Spectrum mixed gas laser was used. The light from the laser was vertically polarized and only vertically polarized light was detected. Since the relaxation time of the photon correlation function is so sensitive to the aggregation state of the sample, it became clear

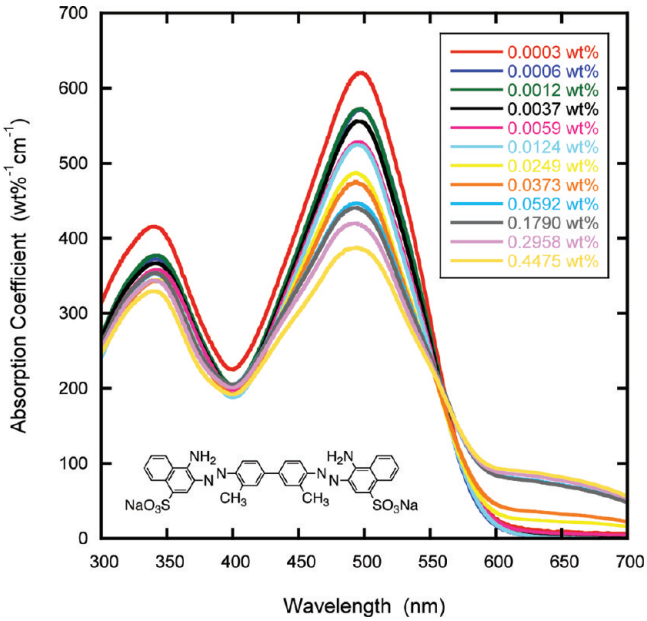

Figure 5. Absorption coefficient for BPP 4B and its dependence on concentration. The structure of BPP 4B is also shown.

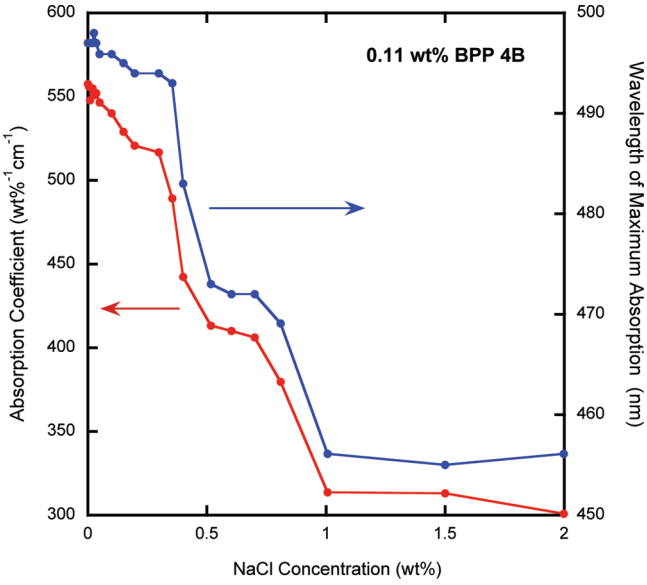

Figure 6. Peak absorption coefficient and wavelength of the peak absorption for BPP 4B with various amounts of added salt.

that BPP 4B takes a long time to equilibrate after a change is made (dilution, heating/cooling, filtering, etc). For that reason, the samples used for light scattering measurements were diluted from a stock solution and allowed to sit for 2 weeks before measurements were taken.

The photon correlation functions for three different concentrations of BPP 4B are shown in Figure 7. At these concentrations the sample is in the isotropic phase. Because the aggregates are not all the same size, the data in Figure 7 do not follow a simple exponential function. A convenient way to extract size information in this case is to fit a stretched exponential function to the data

$$C(t) = C_0 + C_{\text{amp}} e^{-2(t/\tau)^{\beta}} \tag{7}$$

where $C(t)$ is the intensity−intensity correlation function, t is the time, β is the stretching parameter, and C_0 and C_{amp} are

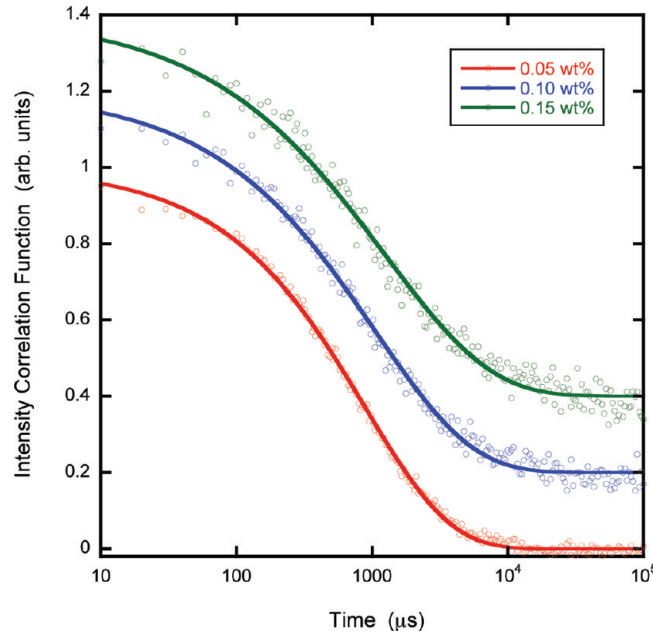

Figure 7. Dynamic light scattering results for three concentrations of BPP 4B in the isotropic phase for a wavelength of 647 nm and a scattering angle of 90°. The data for two of the concentrations have been offset vertically for better visualization. The lines represent fits to a stretched exponential, eq 7, and the resulting parameters are given in Table 1.

TABLE 1: Dynamic Light Scattering Parameters

concentration (wt %)	τ (ms)	β	$\langle t \rangle$ (ms)	$\sigma/\langle t \rangle$
0.05	2.42 ± 0.03	0.70 ± 0.01	3.06	0.75
0.10	3.31 ± 0.09	0.61 ± 0.02	4.88	0.99
0.15	4.37 ± 0.18	0.56 ± 0.02	7.24	1.16

constants. As the polydispersity of the distribution increases, β decreases from 1. Once values of τ and β have been determined, the average relaxation time and the standard deviation of the distribution of relaxation times can be calculated from the moments of the electric field correlation function

$$\langle t^n \rangle = \frac{\tau^n}{\beta} \frac{\Gamma(n/\beta)}{\Gamma(n)} \tag{8}$$

where $\langle t^n \rangle$ is the nth moment of the electric field correlation function and Γ is the Gamma function. The results of this analysis are shown in Table 1, where one of the columns is $\sigma/\langle t \rangle$, the standard deviation of the relaxation time distribution divided by the average relaxation time. The fact that this ratio is close to 1 means that the size distribution is extremely broad, as predicted by theory.

Confocal Microscopy. Samples to be viewed in the confocal microscope were prepared from a 0.81 wt % BPP 4B solution, which is in the liquid crystal phase at room temperature. The solution was forced through a 0.2 μm nylon filter to break up the aggregates so they could form again and to eliminate any larger aggregates or particulates that might be present. This filtering process reduced the concentration by only a small amount (less than 10%), indicating that almost all of the BPP 4B passed through the filter, probably as a result of aggregate breakup. A very small amount of this BPP 4B solution was placed on a microscope slide and a coverslip was dropped on top. Epoxy was applied around the coverslip to seal the sample.

Confocal images were made using a Leica SP5 confocal microscope with 514 nm incident light and detecting emitted

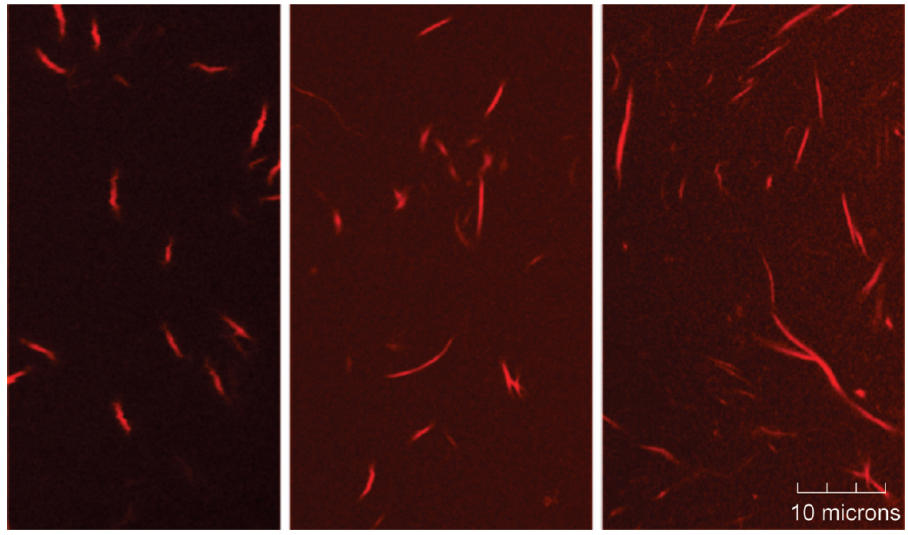

Figure 8. Confocal microscope images of the aggregates of BPP 4B. From left to right, the images were taken 1 day, 1 week, and 2 weeks after filtration of a 0.81 wt % solution.

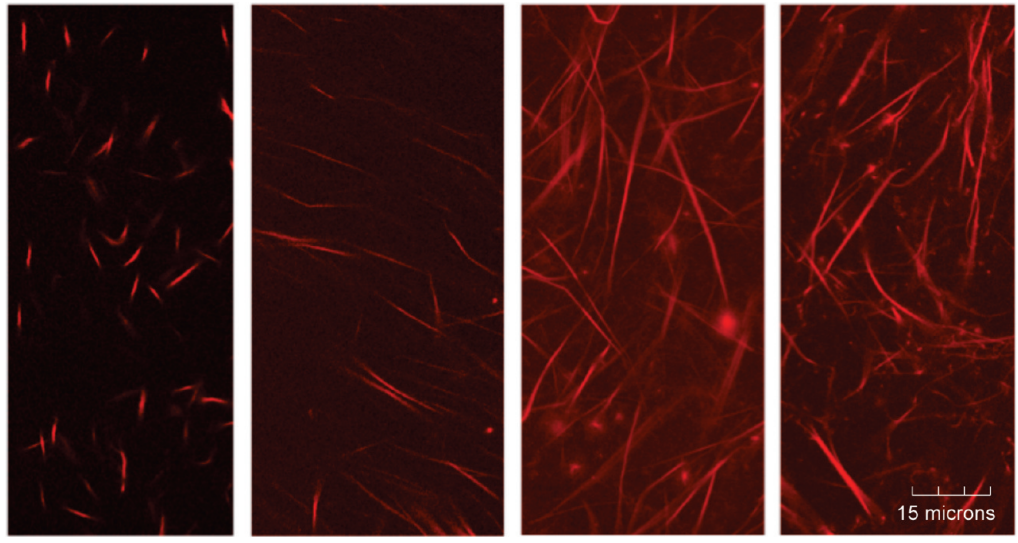

Figure 9. Confocal microscope images of the aggregates of BPP 4B with ethidium bromide added immediately after filtration. From left to right, the images were taken 1 day, 6 days, 8 days, and 13 days after filtration of a 0.81 wt % solution.

light around 600 nm. An oil immersion objective with a numerical aperture of 1.4 was utilized, resulting in a minimum resolution of about 0.2 μm. This was verified by imaging CdSe/ZnS nanocrystals that have a diameter of about 0.005 μm, which produced images with a full-width-half-maximum intensity profile of about 0.4 μm. The entire field of view was quite bright, due to the closely packed aggregates that could not be resolved due to their Brownian motion. However, some aggregates could be imaged because they did not move. Most probably, these are aggregates that were stuck to the glass. This was confirmed by scanning the focus vertically, where these fixed aggregates were only visible when the focus was near either of the inner surfaces of the glass or coverslip.

Figure 8 shows three confocal images that result from this procedure. The solution is the same for all three images, the only difference is the time after filtration (1 day, 1 week, 2 weeks). Since ethidium bromide is known to intercalate between the base pairs of DNA and fluoresce more strongly, and has been shown to intercalate into the aggregates of one liquid crystal,[24] a solution of ethidium bromide was added to a filtered BPP 4B solution so that there were equal molar amounts of BPP 4B and ethidium bromide. The new solution was vortexed and allowed to sit before taking confocal images. Figure 9 contains confocal images of one such solution at four different times after the solution was prepared. The presence of ethidium bromide did enhance the image contrast considerably.

X-ray Scattering. Many chromonic liquid crystals have been examined through X-ray scattering, and just about all of them show a peak corresponding to 3.4 Å, which has been interpreted as due to the stacking of the polyaromatic portions of the molecules.[3] To examine BPP 4B, X-ray diffraction measurements utilized the Cu Kα radiation from a Bruker-Nonius FR591 generator with mirror-monochromator optics and a multiwire detector. The samples were contained in sealed quartz capillary tubes held at room temperature, and experiments were done with both a water sample and a sample of about 6 wt % BPP 4B. The X-ray scattering results are shown in Figure 10. Even at this concentration, the difference between the scattering from water and BPP 4B is small, but a peak at 1.84 Å^{-1} is clearly present, corresponding to a repeat distance of 3.4 Å. There is also some evidence for peaks at lower values of the scattering wavevector, possibly indicating intramolecular correlations of some sort such as a helical pitch.

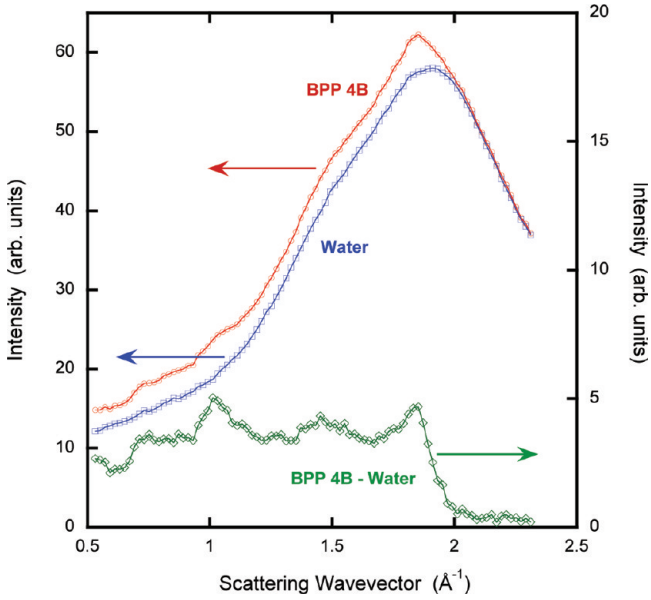

Figure 10. X-ray scattering from a sample of water and a sample of BPP 4B (concentration about 6 wt %). Conditions for the two experiments were identical except for a small difference between the size of the quartz capillary tubes that held the samples. The scattering from water has been slightly scaled to agree with the scattering from BPP 4B at the highest wavevectors. The difference between the scattering from BPP 4B and water is also shown on an expanded scale. The peak at 1.84 Å^{-1} corresponds to the 3.4 Å stacking distance between molecules.

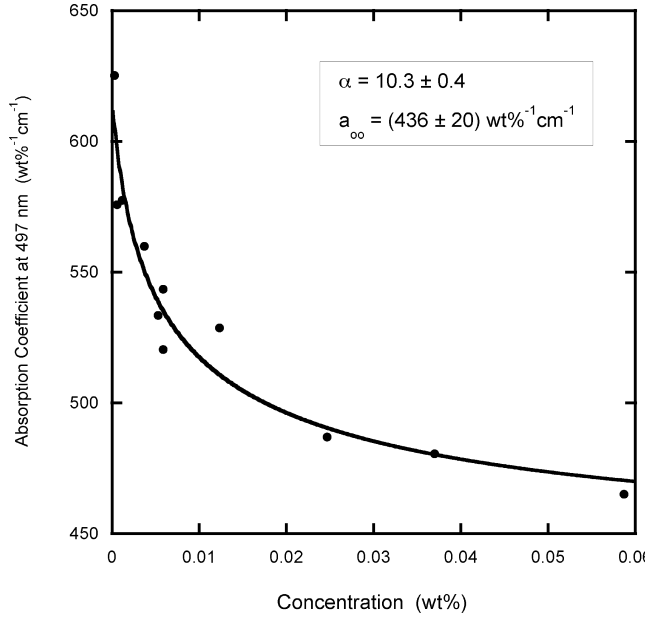

Figure 11. Absorption coefficient for BPP 4B at 497 nm and its dependence on concentration. The line represents a fit to the data of a theory involving isodesmic aggregation and exciton coupling, as explained in the text.

Perhaps more important, no reflection peak was evident at very small angles of scattering. In many chromonic liquid crystal systems, a broad peak is present and reflects the aggregate-aggregate distance.[3] The most probable reason for its absence in BPP 4B is because the aggregates are much larger in size, which places these peaks at much smaller, inaccessible angles.

Discussion

The phase diagram shown in Figure 3 is consistent with the prior results of Bykov et al.,[22] in that the increase in the transition temperature with concentration and the width of the coexistence region are similar. A close comparison is difficult, however, since a much wider concentration range was examined in the previous work and therefore the data points are much more widely spaced. What seems to be different is that the increase in the width of the coexistence region with increasing concentration that is evident in Figure 3 is not present in the earlier results. There could be two reasons for this. First, the purification methods used by Bykov et al. are not described. If in fact there was some salt present in the earlier experiments, it could easily have affected the phase diagram. Second, the compound used by Bykov et al. contained cesium as the counterion, whereas the compound used in the results being reported here contained sodium as the counterion.

Bykov et al. did not identify the liquid crystal phase, and the new observations reported here also do not allow for a firm identification. However, there are good reasons to suspect that it is nematic. First, the higher temperature phase in many chromonic systems is a nematic phase. Second, BPP 4B shows many properties reminiscent of pseudoisocyanine, and its liquid crystal phase has been identified as a nematic phase.[25]

Finally, Bykov et al. state that no evidence for the formation of a liquid crystal phase was observed below a BPP 4B concentration of 0.25 wt %. This was too low a concentration and too low a temperature range to be examined in this investigation, but if true, it points to the conclusion that BPP 4B may be similar to pseudoisocyanine, which possesses a critical micelle concentration that keeps the liquid crystal phase from forming below a certain concentration.[25] It is interesting to speculate whether such behavior might be due to a strong scission free energy (high value for δ), since in this case there is a sharp transition from mostly single molecules in solution to a solution of large molecules. In pseudoisocyanine, the liquid crystal phase forms at a concentration only slightly above the critical micelle concentration.[25]

The change in the absorption spectrum with increasing concentration shown in Figure 5 is similar to what is seen in many chromonic liquid crystal systems (see refs 26 and 10 for examples). If isodesmic aggregation is assumed and a simple model for the change in the absorption spectrum based on exciton theory is used, then an estimation for the stacking free energy change α can be made (see ref 10 for details). The result of this procedure is shown in Figure 11, where it is seen that the value for α is 10.3 $\pm$ 0.4, which is in the high range of observed values.[3] What is interesting is that the liquid crystal phase of BPP 4B occurs at a much lower concentration than recently investigated systems,[3] even though the value of α falls within the range of these systems.

It is important for a disclosure to be made about this analysis of the absorption spectrum. Although the change in the absorption spectrum can be understood as due to the beginning stage of forming large aggregates, it is also possible to analyze the changes as simply being caused by the formation of dimers. If one assumes only dimers are being formed and that the absorption spectrum for dimers is different from that of monomers, a fit almost identical to the one shown in Figure 11 is obtained. Dimerization also explains the presence of what looks like an isosbestic point in the data of Figure 5. There is evidence for dimerization in pseudoisocyanine, with the formation of large aggregates coming at higher concentration.[27] Whether caused by the formation of dimers or large aggregates, this change in the absorption spectrum with concentration is

present in just about all chromonic liquid crystal systems. For those with a liquid crystal phase that forms at room temperature for concentrations above 6 wt % or so, there is a correlation between the value of α found by analyzing the absorption spectrum and the concentration at which the liquid crystal phase forms (the higher α is, the lower the liquid crystal concentration is).[3] With a typical value of α but a much lower liquid crystal phase concentration, BPP 4B does not fit into this scheme. This is evidence that BPP 4B may be different in a fundamental way from the recently studied chromonic liquid crystals.

Figures 4 and 6 make it clear that the presence of salt has a significant effect on the aggregation behavior and liquid crystal phase. This is consistent with many other experiments that have documented the effect of salt on chromonic liquid crystals. For most salts, an increase in the transition temperature is observed with increasing salt concentration, as is also true for BPP 4B. What is different in the results reported here is that both the liquid crystal phase diagram and the absorption spectrum are affected very little until the NaCl concentration reaches about 0.3 wt %.

The dynamic light scattering measurements are clear in demonstrating that the aggregates in BPP 4B are large compared to many chromonic liquid crystals systems. For example, dynamic light scattering on one chromonic liquid crystal system yielded relaxation times at least 100 times smaller than found in BPP 4B.[19] The shape of the correlation function indicates that the size distribution must be extremely broad, which is consistent with an exponentially decreasing size distribution. Also the behavior of the correlation function means that the size of the aggregates and the breath of the size distribution increase with increasing concentration in the concentration range below where the liquid crystal phase forms. This is not at all surprising, but it does provide evidence that if a critical micelle concentration is present in BPP 4B, it must be at a concentration less than 0.05 wt %.

The confocal microscope images are extremely interesting. Of course, it must be kept in mind that there is no way to know for sure if the aggregates that stick to the glass are representative of the aggregates in solution. But there is evidence that points to the conclusion that they are (see next paragraph). A much larger area of the image shown on the left in Figure 8 was analyzed to produce a distribution of aggregate lengths. This was done by using standard image processing software to measure the distance between pixels on the ends of each aggregate where the intensity fell to half its value. The results of this procedure are shown in Figure 12. The average length of the aggregates after 1 day is about 2.5 μm, but more interesting, the distribution shows more aggregates of intermediate length than aggregates of shorter length. This is very different from the prediction of the theories previously described, where the number of aggregates decreases roughly exponentially as the aggregate size increases. This could be explained, however, by a higher tendency for larger aggregates to stick to the glass surfaces.

The full-width-half-maximum (fwhm) values of the aggregates were also measured using the same procedure. The average width was 0.411 ± 0.009 μm. This was only slightly larger than the average fwhm measured for 0.005 μm diameter nanocrystals (0.402 ± 0.007 μm), which can be considered the fwhm of the point spread function. Assuming the FWHMs add in quadrature, an extremely approximate estimate for the width of the aggregate is 0.09 ± 0.05 μm. If one calculates the relaxation time in a dynamic light scattering experiment for ellipsoids with a major axis of 2.5 μm and a minor axis of 0.09 μm, the result is 4.3 ms, which is consistent with the results obtained from dynamic light scattering. While this consistency between the dynamic light scattering and confocal microscope results lends support to the argument that the images did capture a representative sample of the aggregates present, the standard deviation divided by the average length for the size distribution of Figure 12 is much less than the corresponding relaxation time ratios given in Table 1.

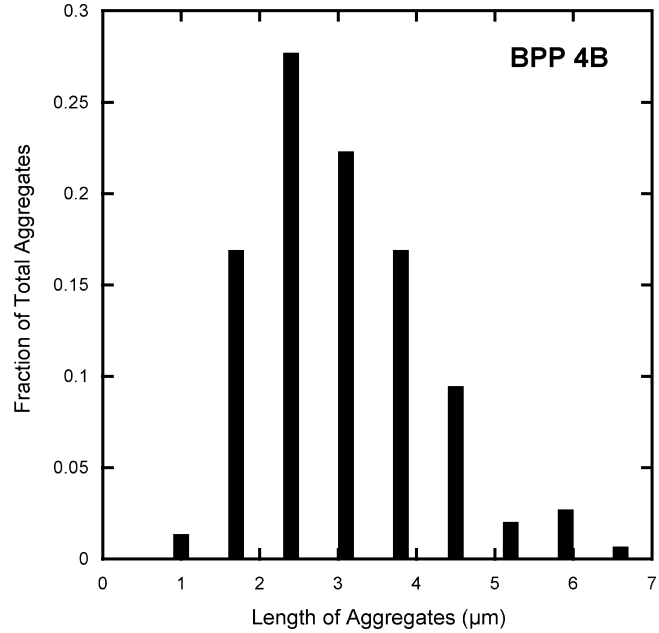

Figure 12. Distribution of aggregate lengths in a single confocal microscope image taken one day after preparing the 0.81 wt % BPP 4B sample.

It is interesting to compare the images with and without ethidium bromide added. It is clear from Figures 8 and 9 that besides enhancing the contrast of the images, ethidium bromide affects the aggregation by increasing the length of the aggregates while maintaining the same width (with the understanding that the width in both cases is basically the same as the point spread function). This increase in length is small at first. For example, a full analysis of the distribution of lengths 1 day after sample preparation produces a histogram very similar to Figure 12, but with an average length of about 3.0 μm instead of 2.5 μm. But after a week or so, the aggregates with ethidium bromide are considerably longer than those without ethidium bromide.

An X-ray peak corresponding to a repeat distance of 3.4 Å demonstrates that molecular stacking is the basic structure for BPP 4B aggregates as it is for other chromonic liquid crystals. The absence of X-ray peaks at smaller angles, as is seen in other systems, is additional evidence that the aggregates in BPP 4B are larger, although the reason may also be due to the low concentration used. A lower bound estimate on the distance between aggregates from confocal microscopy is 0.09 μm, which would produce an upper bound estimate for the X-ray reflection of 0.007 $Å^{-1}$. This represents too small an angle to be observed in the X-ray apparatus used.

Conclusions

Taken altogether, the evidence is extremely strong that the aggregates formed by BPP 4B in aqueous solution are much larger than one finds in the chromonic liquid crystals recently studied. Thus in some sense, BPP 4B may be more similar to systems such as pseudoisocyanine, in which large aggregates

and a liquid crystal phase form at very low concentrations. Since there must be considerable interactions between aggregates for an organized liquid crystal phase to form, and since there is very little dye in the system with which to construct these interacting aggregates, it is extremely likely that the BPP 4B aggregates incorporate water, perhaps in the"hollow cylinder" structure hypothesized for some cyanine dyes.[20] This is in line with NMR measurements on BPP 4B, which show that a considerable fraction of the water is not free.[22]

Acknowledgment. The partial support of this work by the Petroleum Research Fund of the American Chemical Society is acknowledged, as is additional support from the Howard Hughes Medical Institute and the Research Experiences for Undergraduates Program at the Laboratory for Research in the Structure of Matter at the University of Pennsylvania. The valuable assistance of Catherine Crouch, Mihai Peterca, and Jessica Gersh is also gratefully acknowledged.

References and Notes

(1) Lydon, J. *Curr. Opin. Colloid Interface Sci.* **1998**, *3*, 458.
(2) Lydon, J. *Curr. Opin. Colloid Interface Sci.* **2004**, *8*, 480.
(3) Dickinson, A. J.; LaRacuente, N. D.; McKitterick, C. B.; Collings, P. J. *Mol. Cryst. Liq. Cryst.* **2009**, *509*, 751.
(4) Park, H. S.; Kang, S. W.; Tortora, L.; Nastishin, Y.; Finotello, D.; Kumar, S.; Lavrentovich, O. D. *J. Phys. Chem. B* **2008**, *112*, 16307.
(5) Edwards, D. J.; Jones, J. W.; Lozman, O.; Ormerod, A. P.; Sintyureva, M.; Tiddy, G. J. T. *J. Phys. Chem. B* **2008**, *112*, 14628.
(6) Prasad, S. K.; Nair, G. G.; Hegde, G.; Jayalakshmi, V. *J. Phys. Chem. B* **2007**, *111*, 9741.
(7) Tortora, L.; Park, H. S.; Antion, K.; Finotello, D.; Lavrentovich, O. D. *Proc. SPIE* **2007**, *6487*, 6487OI-1.
(8) Boikov, O. P.; Vasyuta, R. M.; Nazarenko, V. G.; Pergamenshchik, V. M.; Nastishin, Y. A.; Lavrentovich, O. D. *Mol. Cryst. Liq. Cryst.* **2007**, *467*, 181.
(9) Kaznacheev, K. V.; Dudin, P.; Lavrentovich, O. D.; Hitchcock, A. P. *Phys. Rev. E* **2007**, *76*, 061703.
(10) Tomasik, M. R.; Collings, P. J. *J. Phys. Chem. B* **2008**, *112*, 9883.
(11) Mobius, D. *Adv. Mater.* **1995**, *7*, 437.
(12) von Berlepsch, H.; Bottcher, C.; Dahne, L. *J. Phys. Chem. B* **2000**, *104*, 8792.
(13) Neumann, B. *J. Phys. Chem. B* **2001**, *105*, 8268.
(14) Collings, P. J.; Gibbs, E. J.; Starr, T. E.; Vafek, O.; Yee, C.; Pomerance, L. A.; Pasternack, R. F. *J. Phys. Chem. B* **1999**, *103*, 8474.
(15) von Berlepsch, H.; Bottcher, C. *J. Phys. Chem. B* **2002**, *106*, 3146.
(16) Kostko, A. F.; Cipriano, B. H.; Pinchuk, O. A.; Ziserman, L.; Anisimov, M. A.; Danino, D.; Raghavan, S. R. *J. Phys. Chem. B* **2005**, *109*, 19126.
(17) Pasternack, R. F.; Fleming, C.; Herring, S.; Collings, P. J.; dePaula, J.; DeCastro, G.; Gibbs, E. J. *Biophys. J.* **2000**, *79*, 550.
(18) Parkash, J.; Robblee, J. H.; Agnew, J.; Gibbs, E.; Collings, P.; Pasternack, R.; dePaula, J. C. *Biophys. J.* **1998**, *74*, 2089.
(19) Betrand, C. E.; Linegar, K. L.; Kostko, A. F.; Anisimov, M. A. *Phys. Rev. E* **2009**, *79*, 041704.
(20) Harrison, W. J.; Mateer, D. L.; Tiddy, G. J. T. *J. Phys. Chem. B* **1996**, *100*, 2310.
(21) Edwards, D. J.; Ormerod, A. P.; Tiddy, G. J. T.; Jaber, A. A.; Mahendrasingham, A. *Adv. Color Chem. Ser.* **1996**, *4*, 83.
(22) Bykov, V. A.; Sharimanov, Y. G.; Mrevlishvili, G. M.; D. Mdzinarashvili, T.; Metreveli, N. O.; Kakabadze, G. R. *Mol. Mat.* **1992**, *1*, 73.
(23) Gelbart, W. M.; Ben-Shaul, A. *J. Phys. Chem.* **1996**, *100*, 13169.
(24) Mundy, K.; Sleep, J. C.; Lydon, J. E. *Liq. Cryst.* **1995**, *19*, 107.
(25) Stegemeyer, H.; Stockel, F. *Ber. Bunsen-Ges. Phys. Chem.* **1996**, *100*, 9.
(26) Horowitz, V. R.; Janowitz, L. A.; Modic, A. L.; Heiney, P. A.; Collings, P. J. *Phys. Rev. E* **2005**, *72*, 041710.
(27) Kopainsky, B.; Hallermeier, J. K.; Kaiser, W. *Chem. Phys. Lett.* **1981**, *83*, 498.

JP910136P